# Novel Cu Nanowires/Graphene as the Back Contact for CdTe Solar Cells

*Jun Liang, Hui Bi, Dongyun Wan,* and Fuqiang Huang**

**Cu-nanowire-doped graphene (Cu NWs/graphene) is successfully incorporated as the back contact in thin-film CdTe solar cells. 1D, single-crystal Cu nanowires (NWs) are prepared by a hydrothermal method at 160 °C and 3D, highly crystalline graphene is obtained by ambient-pressure CVD at 1000 °C. The Cu NWs/graphene back contact is obtained from fully mixing the Cu nanowires and graphene with poly(vinylidene fluoride) (PVDF) and *N*-methyl pyrrolidinone (NMP), and then annealing at 185 °C for solidification. The back contact possesses a high electrical conductivity of 16.7 S cm$^{-1}$ and a carrier mobility of 16.2 cm$^2$ V$^{-1}$ s$^{-1}$. The efficiency of solar cells with Cu NWs/graphene achieved is up to 12.1%, higher than that of cells with traditional back contacts using Cu-particle-doped graphite (10.5%) or Cu thin films (9.1%). This indicates that the Cu NWs/graphene back contact improves the hole collection ability of CdTe cells due to the percolating network, with the super-high aspect ratio of the Cu nanowires offering enormous electrical transport routes to connect the individual graphene sheets. The cells with Cu NWs/graphene also exhibit an excellent thermal stability, because they can supply an active Cu diffusion source to form an stable intermediate layer of CuTe between the CdTe layer and the back contact.**

## 1. Introduction

The CdTe thin-film solar cell is a leading technology for next-generation energy products.[1] The First Solar Corporation announced the highest efficiency by far of 17.3%, which was confirmed by the National Renewable Energy Laboratory (NREL).[2] The cell performances and service stability are extremely important, and are strongly dependent on the characteristics of the back contact.[3,4] Much effort has been devoted to introducing Cu into CdTe thin films[5] and developing Cu-based back contact materials.[6,7] Cu diffusion to the surface of CdTe absorbers plays a significant role in improving the performance of CdTe solar cells by forming ohmic back contacts. Conventional methods use Cu thin films (Cu TFs) followed by a thick Ni layer (as an electrode), or graphite paste containing Cu particles (Cu Ps, ≈75 μm in diameter) as a thermal diffusion source to the CdTe layer, to form a $Cu_xTe$ intermediate layer (typically $x$ = 1.44 at relatively low annealing temperatures). However, it is difficult to form a stable $Cu_xTe$ phase (e.g., $x$ = 1) under the thermal limitations during cell fabrication with Cu TFs or large-size Cu Ps. A large amount of free Cu can diffuse into the CdS/CdTe PN junction, which greatly affects the cell performance.[8,9] Low-dimensional nanowires (NWs), with a large specific surface area, are desirable as excellent doping materials at low temperature.[10–13]

Although a doped graphite back contact can stand as a barrier for Cu diffusion,[14,15] graphite has a relatively low conductivity due to its anisotropic electrical conduction. The conductivity perpendicular to the graphite layer is ≈50 S cm$^{-1}$, much smaller than the in-plane conductivity (10$^6$ S cm$^{-1}$),[16] resulting in low carrier collection and a high resistance of the cell back contact.[6] Single- or few-layer graphene has excellent electrical transport properties:[17–20] graphene from chemical vapor deposition (CVD) possesses extremely high carrier mobility up to 20 000 cm$^2$ V$^{-1}$ s$^{-1}$.[21–23] Therefore, graphene is more suitable than graphite to collect carriers (electrons and holes) for CdTe solar cells. We recently explored graphene as the front and back electrode applied in CdTe solar cells, and their efficiencies reached 4.15% and 7.86%, respectively.[24,25] However, integrated graphene-based back contacts still show poor electrical characteristics due to the large resistance from the interface of the sub-micrometer graphene sheets and its compatibility to the CdTe absorber. Therefore, large-size, highly conductive graphene with an effective dopant is demanded for high-efficiency CdTe applications.

In this paper, we propose a novel back contact structure of 1D Cu-nanowire-doped graphene (Cu NWs/graphene) applied in CdTe solar cells. 1D, single-crystal Cu NWs were prepared via a hydrothermal method and then doped into large-size, high-quality graphene, which was obtained using a 3D Ni foam catalyst by ambient-pressure CVD (APCVD). CdTe solar cells based on the Cu NWs/graphene back contact show an excellent cell performance with regard to photovoltaic efficiency and

Dr. J. Liang, Dr. H. Bi, Dr. D. Y. Wan, Prof. F. Q. Huang
CAS Key Laboratory of Materials for Energy Conversion
Shanghai Institute of Ceramics
Chinese Academy of Sciences
Shanghai 200050, P. R. China
E-mail: wandy@mail.sic.ac.cn; huangfq@mail.sic.ac.cn
Prof. F. Q. Huang
College of Chemistry and College of Engineering
Peking University
Beijing 100871, P. R. China

DOI: 10.1002/adfm.201102809


© 2012 WILEY-VCH Verlag GmbH & Co. KGaA, Weinheim

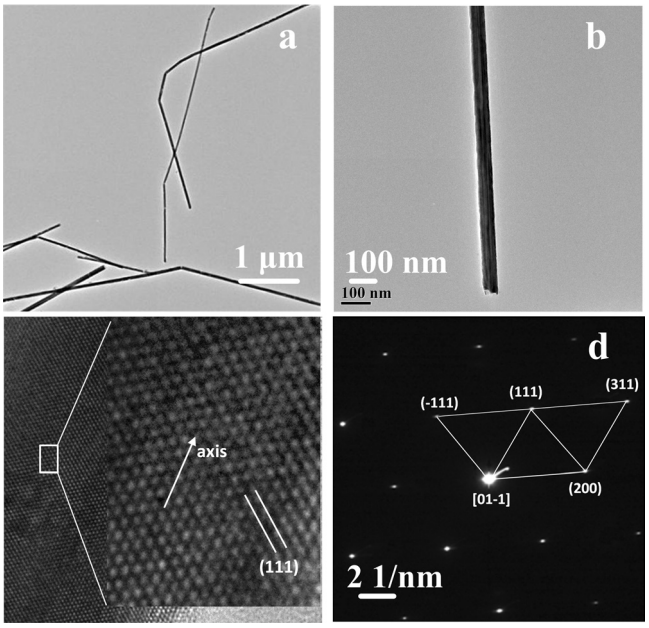


**Figure 1.** a,b) Low-magnification (a) and high-magnification (b) TEM images of the 1D Cu NWs. c–d) HR-TEM (c) and SAED (d) patterns of a single-crystal Cu nanowire.

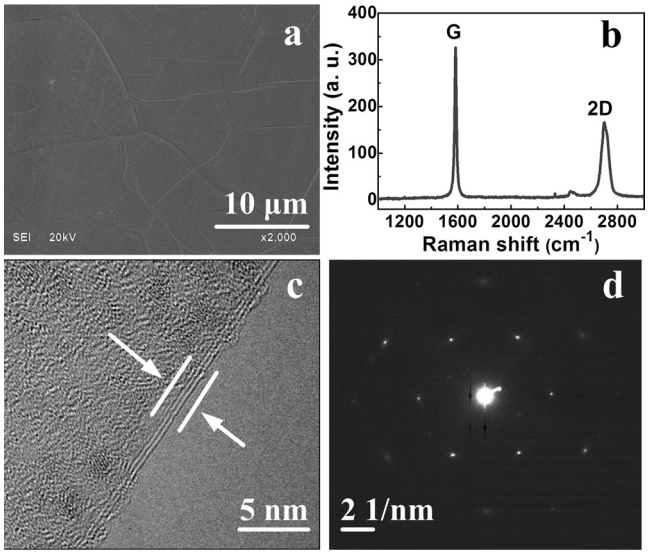


**Figure 2.** a) Top-view SEM image of graphene on Ni foam via APCVD. b–d) Raman spectrum (b), TEM image (c), and SAED pattern (d) of the triple-layer graphene.

a thermal stability that is superior to those of traditional back contacts of Cu-doped graphite and Cu-TFs.

## 2. Results and Discussion

### 2.1. Microstructure Characterization Investigation

1D Cu NWs were obtained by a hydrothermal process by adding 2 mmol of octadecylamine and 1 mmol of $CuCl_2$ into 100 ml of distilled water and reacting them at 160 °C for 48 h: see the Experimental Section for the experimental details. Low- and high-magnification transmission electron microscopy (TEM) images of 1D Cu NWs are shown in **Figure 1**a,b. The Cu NWs were straight with diameters of ≈70 –130 nm, and the extraordinary length was of millimeter magnitude, with an aspect ratio of more than $10^5$. The high-resolution TEM (HR-TEM) image confirms the features of a single-crystal Cu phase. The lattice fringe distance was 2.08 Å, consistent with the Cu (111) interplanar spacing, shown in Figure 1c, and the angle between the (111) plane and the axis was 55°. The spot feature of the corresponding selected area electron diffraction (SAED) pattern (Figure 1d) also confirms that the NWs were single crystal with a face-centered cubic structure.

We explored the APCVD method to deposit large-size graphene sheets of high crystalline quality on 3D Ni foams with $CH_4/H_2/Ar$ at 2/50/300 sccm at 1000 °C. The as-grown graphene, with many wrinkles, fully covered the entire Ni-foam surface after 10 min growth, as shown in **Figure 2**a. The wrinkle formation was due to the thermal expansion coefficient difference between the Ni and the graphene. Suspended graphene, bridging the gaps between the interfacial Ni grains, could cross the crystal boundary of the Ni foam to form continuous, large-size, 3D graphene sheets (≈10–50 μm). After complete 5 M HCl solution etching of the Ni, the graphene was obtained (specific experimental details are described in the Experimental Section). The harvested yield of graphene was typically ≈1–4 wt%, based on the current type of Ni foams in this lab. It is worthy of note that these high yields of graphene can be obtained easily using large Ni-foam substrates, for future applications.

The quality and layer numbers of the as-prepared, 3D, porous graphene were examined using the powerful non-destructive tool of Raman spectroscopy. Two peaks, of the G band (≈1585 $cm^{-1}$) and the 2D band (≈2706 $cm^{-1}$), are shown in Figure 2b. The position, intensity and shape of the 2D band are the most prominent feature of graphene. The shape of 2D band was a broad peak at 2706 $cm^{-1}$, and the $I_{2D}/I_G$ ratio was about 0.5, indicating that the as-grown graphene had around three layers. In addition, HR-TEM further confirmed three-layer graphene (Figure 2c), and the interlayer spacing was calculated as 3.40 Å. The SAED pattern along the (001) direction of the three-layer graphene (Figure 2d) revealed the distinctive hexagonal structure, and the well-indexed diffraction spots further suggest good crystallinity in all regions of the graphene sheets.

A conductive paste of the Cu NWs/graphene was obtained by mixing 1 wt% Cu nanowires with graphene in a solution of 10% poly(vinylidene fluoride) (PVDF) and *N*-methyl pyrrolidinone (NMP), and the paste was eventually dried after annealing in $N_2$ at 185 °C for 30 min. The electrical properties of the Cu NWs/graphene contact were measured through Hall measurements. The electrical conductivity ($\sigma$) of the Cu NWs/graphene was 16.7 S $cm^{-1}$ and the carrier mobility ($\mu$) reached up to 16.2 $cm^2$ $V^{-1}$ $s^{-1}$, much higher than those of Cu Ps/graphene ($\sigma \approx 14.2$ S $cm^{-1}$ and $\mu \approx 13.2$ $cm^2$ $V^{-1}$ $s^{-1}$) and Cu Ps/graphite ($\sigma \approx 5.5$ S $cm^{-1}$ and $\mu \approx 5.0$ $cm^2$ $V^{-1}$ $s^{-1}$) (**Table 1** and Table S1,


© 2012 WILEY-VCH Verlag GmbH & Co. KGaA, Weinheim

**Table 1.** Photovoltaic parameters of the CdTe cells with four different back contacts annealed at 185 °C for 30 min under $N_2$ conditions.

| Back contact material | $\sigma$ [S cm$^{-1}$] | $\mu$ [cm$^2$ V$^{-1}$ s$^{-1}$] | $V_{oc}$ [mV] | $J_{sc}$ [mA cm$^{-2}$] | FF [%] | Eff. [%] |
|---|---|---|---|---|---|---|
| Cu NWs/ graphene | 16.7 | 16.2 | 801 | 22.4 | 67.4 | 12.1 |
| Cu Ps/graphene | 14.2 | 13.2 | 805 | 21.3 | 68.1 | 11.7 |
| Cu Ps/graphite | 5.5 | 5.0 | 790 | 21.2 | 62.5 | 10.5 |
| Cu TF | - | - | 740 | 21.1 | 58.0 | 9.1 |

Supporting Information). The conductive paste of the Cu NWs/graphene can provide a practical application as a special functional back contact in CdTe solar cells.

### 2.2. Cu NWs/Graphene as the Back Contact of Solar Cells

CdTe cells were fabricated on $SnO_2$:F glass (fluorine-doped tin oxide (FTO)) with the structure of FTO/CdS/CdTe/Cu NWs/graphene. The fabrication is described in the Experimental Section, and the solar cell is shown schematically in **Figure 3**a. For comparison, cells were also made with back contacts of Cu Ps/graphene, Cu Ps/graphite and Cu TF. Figure 3b shows the schematic band structure of a back contact with a $Cu_xTe$ intermediate layer. After chemical mechanical polishing of back contacts of Cu NWs/graphene, Cu Ps/graphene, Cu Ps/graphite or Cu TF, the $Cu_xTe$ intermediate layer on the surface of the CdTe absorbers was exposed. The microstructure of the surface area was analyzed by X-ray diffraction (XRD) measurements with a 0.5°-angle incidence, as shown in Figure 3c. The $Cu_xTe$ intermediate layer attached to Cu NWs/graphene exhibited a CuTe phase with a preferred [001] peak, while those attached to the other three Cu-doped back contacts showed a $Cu_{1.44}Te$ phase with a [002] peak. The corresponding quantum efficiencies (QEs) of the CdTe solar cells are shown in Figure 3d. The cell with Cu NWs/graphene had a more-sensitive response in the visible light range of ≈560 –685 nm, and the peak of the QE reached 86.5% at 620 nm. The QE peak of the cell with Cu Ps/graphene appeared at the same position, but its intensity was reduced to 85.2%. In the cases of Cu Ps/graphite and Cu TF, no such obvious response peak appeared. The high QE in the visible-light range may be attributed to the highly conductive Cu NWs/graphene, which can effectively collect holes from the CdTe absorber, due to the formation of CuTe (CuTe is a better hole collector than $Cu_{1.44}Te$).

The photocurrent-density–voltage ($J$–$V$) characteristics of the cells with the different back contacts were estimated by photovoltaic efficiency measurements, as shown in Figure 3e. All of the cells showed a good contact, following ohmic conductivity. The efficiency of the cell with Cu NWs/graphene was 12.1%, higher than those of the Cu Ps/graphene (11.7%), Cu Ps/graphite (10.5%) and Cu TF (9.1%), and the detailed photovoltaic parameters are listed in Table 1. Both of the cells with Cu-doped graphene were better than that with Cu in graphite, confirming that graphene possesses a high capacity to collect holes. For the efficiency of the cells with Cu in graphene, that of the cell with the NWs was a little higher than that of the cell with the Ps, due to a high short-circuit current density ($J_{sc}$).

The high $J_{sc}$ of the cells with Cu NWs/graphene relates to the hole collection of the back contact. One reason is that the 3D NW network built up by the graphene supplies a more effective hole-transportation channel.[26,27] Another reason is from the interface between the CdTe layer and the back

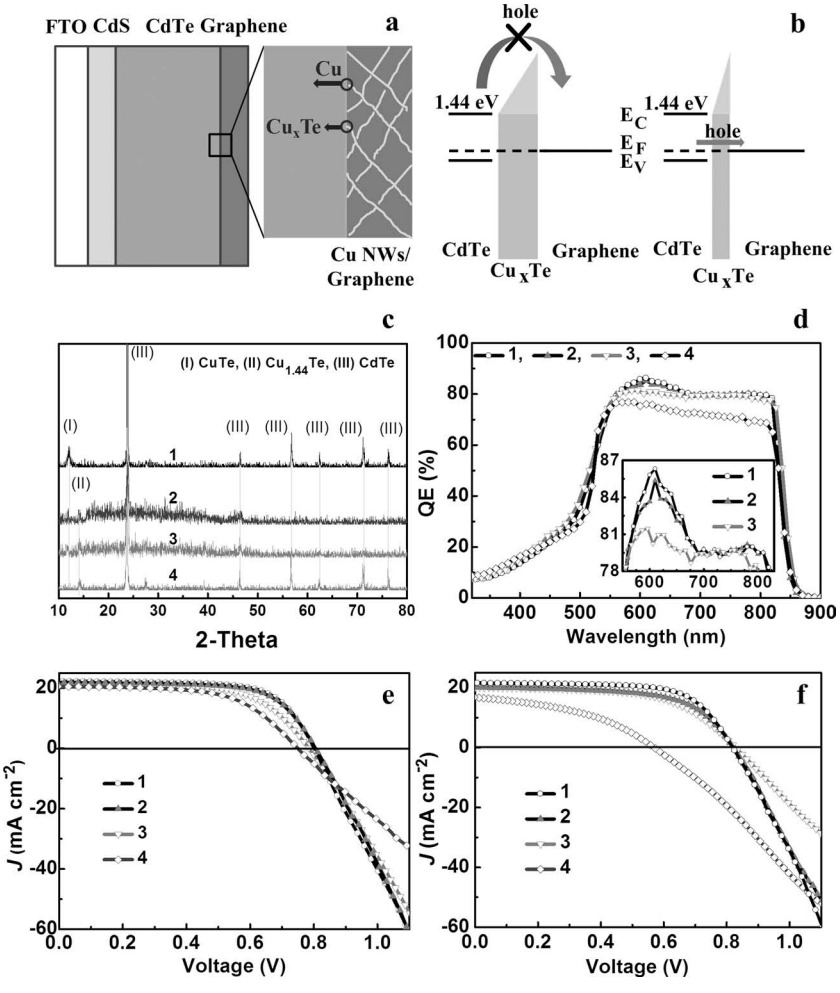


**Figure 3.** a,b) The schematic solar cell (a) and the band structure of FTO/CdS/CdTe/Cu NWs/graphene (b). c) XRD patterns of the surface CdTe absorber annealed at 185 °C with Cu NWs/graphene (1), Cu Ps/graphene (2), Cu Ps/graphite (3) and Cu TF (4). d) The corresponding QE of the CdTe solar cells, and the visible-light QE in the inset. e–f) $J$ – $V$ characteristics of the CdTe solar cells before (e) and after (f) thermal stress.


© 2012 WILEY-VCH Verlag GmbH & Co. KGaA, Weinheim

contact. According to its band structure (Figure 3b), there are two conduction mechanisms in the back contact: one is thermal electron emission (TEE) conduction and the other is tunnel current conduction. In the dominance of TEE conduction, for avoidance of a Schottky barrier, the back contact is required to have a higher work function than CdTe for the formation of an ohmic contact. However, the work function of CdTe is 5.5 eV, which is higher than that of graphene/graphite (≈4.6 eV), and few conductive materials meet the requirement.[28,29] It is a feasible solution to supply a tunnel to transport holes at the interface between the CdTe layer and the back contact, through the $Cu_xTe$ interface layer. A $Cu_xTe$ phase with $x > 1.4$ is unstable.[30] With the NWs/graphene as the back contact, the Cu NWs with a 1D $\phi$ of 100 nm have a larger specific surface area than that of the Cu Ps (≈75 μm). The Cu NWs annealed at 185 °C for 30 min can react effectively with sufficient Te atoms to form a stable intermediate CuTe layer. Although the barrier still exists, the tunnel current conduction mechanism becomes dominant, in which the tunnel current increases sharply and overcomes hole loss from the barrier. The other back contacts, including to Cu Ps/graphene, Cu Ps/graphene and Cu TF, were annealed at 185 °C to form $Cu_{1.44}Te$, due to insufficient Te source material and the relatively low annealing temperature: this is the undesirable phase for high-efficiency and stable CdTe solar cells.

### 2.3. Thermal Stability of Cells with 1D NWs/Graphene

In order to evaluate the stability of the NWs/graphene back contact, we accelerated the degradation of the cells by annealing them in $N_2$ at 185 °C for 120 min to compare the *J–V* characteristics with those of the other back contacts (Table S1, Supporting Information and Figure 3f). The cell efficiency with Cu TFs degraded rapidly from 9.1% to 4.2%. The cell efficiency with the Cu Ps/graphene and that with the Cu Ps/graphite degraded from 11.7% to 10.0% and from 10.5% to 9.2%, respectively. The cell with the Cu NWs/graphene showed much-better stability with a small efficiency loss from 12.1% to 11.6%.

After thermal stress for 120 min, the deterioration of the cells with Cu TFs was derived from the large amount of free Cu access, deep into the CdTe/CdS PN junction.[3] For the graphite- or graphene-containing back contacts, Cu diffusion is restricted to the barrier of the graphite or graphene and has no such severe deterioration of the cell performances.[6,31] The stability of the cells with Cu NWs/graphene was superior to that of those with Cu Ps/graphene and Ps/graphite. Cu derived from the Cu NWs formed a stable CuTe intermediate layer during the 185 °C, 30min annealing. In the other back contacts, the as-formed $Cu_{1.44}Te$ layer was unstable, and some Cu atoms penetrated into the PN junction via the thermal field that was applied for 120 min to deteriorate the thermal stability of the solar cells.

## 3. Conclusions

In summary, we have developed a novel CdTe back contact structure with 1D Cu NWs/graphene for the improvement of solar cells. 1D, single-crystal Cu NWs were prepared via a hydrothermal method and high-quality, large-size graphene was obtained by pyrolysis of methane using a 3D Ni-foam catalyst. The electrical conductivity of the Cu NWs/graphene was 16.7 S $cm^{-1}$ and the carrier mobility was 16.2 $cm^2$ $V^{-1}$ $s^{-1}$. The Cu NWs/graphene as a back contact exhibited a high hole collection ability; the short-circuit current density of the cell reached 22.4 mA $cm^{-2}$, and the photovoltaic efficiency was up to 12.1%. The thermal stability of the cells also benefitted from the 1D Cu NWs/graphene, and was attributed to the formation of stable CuTe at the interface of the Cu NWs and the CdTe layer. The conductive paste of the 1D Cu NWs/graphene provided a feasible application for highly efficient and thermally stable solar cells.

## 4. Experimental Section

*Preparation of Cu NWs*: 2 mmol of octadecylamine (ODA) and 1 mmol of $CuCl_2$ were added to 100 mL of distilled water and stirred for 5 h to form a blue emulsion. Then, the solution was heated at 160 °C for 48 h. After cooling down naturally to room temperature, the supernatant was decanted, and the final product was obtained after washing with hexane, ethanol and deionized (DI) water, in that order. After drying, 1D Cu NWs were obtained.

*Preparation of Graphene*: A Ni-foam substrate was placed in a quartz tube with a flow of hydrogen ($H_2$) (50 sccm) and argon (Ar) (300 sccm). When the furnace temperature reached at 1000 °C, 2 sccm $CH_4$ gas was introduced into the flow as the carbon source for CVD. After the 10 min CVD growth, the furnace was cooled to room temperature under ambient $H_2$, and the detailed profile was obtained (Figure S1, Supporting Information). A thin poly(methyl methacrylate) (PMMA) layer was deposited on the graphene surface as a support to prevent the graphene architecture from collapsing during etching of the Ni-foam. The sample was transferred to a 5 M HCl solution until the Ni was completely etched. Finally, the PMMA layer was dissolved with acetone to yield a large-sized graphene sheet, and Ni-free graphene was confirmed by energy dispersive X-ray spectroscopy (EDS) measurements (Figure S2, Supporting Information).

*Fabrication of FTO/CdS/CdTe/Cu NWs-graphene*: The FTO glass substrate was firstly cleaned by sonication in a 1% solution of Liquinox soap, followed by acetone, isopropyl alcohol and deionized water. A 200 nm-thick CdS layer was deposited on the FTO glass via chemical bath deposition (CBD) at 88 °C. A 7 μm CdTe layer was deposited by close-space sublimation (CSS) at 580 °C under a flow of 85% Ar + 15% $O_2$. Thermal treatment with a $CdCl_2$ coating at 420 °C for 30 min under $N_2$ conditions, and then etching in a 88:1:35 phosphoric acid:nitric acid:DI-water (NP etch) mixture for 30 s at room temperature, were carried out to provide a clean Te-rich surface to the CdTe layer. A paste of Cu-nanowire-doped graphene (Cu NWs/graphene) was brushed on the surface of the CdTe layer of the cell, and then the cell was annealed in $N_2$ at 185 °C for 30 min. Finally, a thin layer of silver paste was applied to the back contact, and the cells were scribed to 1 cm × 0.5 cm area. For comparison, CdTe cells with Cu-Ps-doped graphene (Cu Ps/graphene) and Cu-Ps-doped graphite (Cu Ps/graphite) as back contacts were fabricated to follow the same process. The CdTe cells with a 5 nm-thick Cu thin film followed by a Ni layer as the back contact were also made as a reference.

## Supporting Information

Supporting Information is available from the Wiley Online Library or from the author.


© 2012 WILEY-VCH Verlag GmbH & Co. KGaA, Weinheim

## Acknowledgements

J.L. and H.B. contributed equally to this work. Financial support from the National 973 & 863 Program of China (Grant Nos. 2009CB939903 & 2011AA050505), the NSF of China (Grant Nos. 91122034, 51125006, 50821004, 61106088, 21101164, 61076062 & 51102263), and the Science and Technology Commission of Shanghai (Grant Nos. 10520706700 & 10JC1415800) is acknowledged.

Received: November 21, 2011
Published online: January 19, 2012

[1] K. Zweibel, *Science* **2010**, *328*, 699.
[2] http://investor.firstsolar.com/releasedetail.cfm?ReleaseID=593994 (accessed Janary 2012).
[3] H. Lin, W. Xia, H. N. Wu, C. W. Tang, *Appl. Phys. Lett.* **2010**, *97*, 123504.
[4] A. Nimegeers, M. Burgelmann, *J. Appl. Phys.* **1997**, *81*, 2881.
[5] E. D. Jones, N. M. Stewart, J. B. Mullin, *Adv. Funct. Mater.* **1994**, *1*, 209.
[6] D. H. Rose, F. S. Hasoon, R. G. Dhere, D. S. Albin, R. M. Ribelin, X. S. Li, Y. Mahathongdy, T. A. Gessert, P. Sheldon, *Prog. Photovoltaics: Res. Appl.* **1999**, *7*, 331.
[7] X. Wu, J. Zhou, A. Duda, Y. Yan, G. Teeter, S. Asher, W. K. Metzger, S. Demtsu, S. H. Wie, R. Noufi, *Thin Solid Films.* **2007**, *515*, 5798.
[8] S. H. Demtsu, D. S. Albin, J. W. Pankow, A. Davies, *Sol. Energy Mater. Sol. Cells.* **2006**, *90*, 2934.
[9] W. Jaegermann, A. Klein, T. Mayer, *Adv. Mater.* **2009**, *21*, 4196.
[10] M. E. Toimil Molares, E. M. Hohberger, C. Schaeflein, R. H. Blick, R. Neumann, C. Trautmann, *App. Phys. Lett.* **2003**, *82*, 2139.
[11] L. Lu, Y. F. Shen, X. H. Chen, L. H. Qian, K. Lu, *Science.* **2004**, *304*, 422.
[12] G. D. Zhan, J. D. Kuntz, J. L. Wan, A. K. Mukherjee, *Nat. Mater.* **2003**, *2*, 38.
[13] N. Varghese, K. Vinod, S. Rahul, K. M. Devadas, S. Thomas, S. Pradhan, U. Syamaprasad, *J. Appl. Phys.* **2011**, *109*, 033902.
[14] M. H. Du, *Phys. Rev. B: Condens. Matter* **2009**, *80*, 205322.
[15] S. Pookpanratana, X. Liu, N. R. Paudel, L. Weinhardt, M. Bar, Y. Zhang, A. Ranasinghe, F. Khan, M. Blum, W. Yang, A. D. Compaan, C. Heske, *Appl. Phys. Lett.* **2010**, *97*, 2109.
[16] K. S. Krishnan, N. Ganguli, *Nature* **1939**, *144*, 667.
[17] K. S. Novoselov, A. K. Geim, S. V. Morozov, D. Jiang, M. I. Katsnelson, I. V. Grigorieva, S. V. Dubonos, A. A. Firsov, *Nature* **2005**, *438*, 197.
[18] A. K. Geim, K. S. Novoselov, *Nat. Mater.* **2007**, *6*, 183.
[19] D. A. Dikin, S. Stankovich, E. J. Zimney, R. Piner, G. H. B. Dommett, G. Evmenenko, S. T. Nguyen, R. S. Ruoff, *Nature* **2007**, *448*, 457.
[20] M. F. Craciun, S. Russo, M. Yamamoto, J. B. Oostinga, A. F. Morpurgo, S. Tarucha, *Nat. Nanotechnol.* **2009**, *4*, 383.
[21] Y. Wang, S. W. Tong, X. F. Xu, B. Özyilmaz, K. P. Loh, *Adv. Mater.* **2011**, *23*, 1514.
[22] X. Li, H. Zhu, K. Wang, A. Cao, J. Wei, C. Li, Y. Jia, Z. Li, X. Li, D. Wu, *Adv. Mater.* **2010**, *22*, 2743.
[23] Y. Ye, Y. Dai, L. Dai, Z. Shi, N. Liu, F. Wang, L. Fu, R. Peng, X. Wen, Z. Chen, Z. Liu, G. Qin, *ACS Appl. Mater. Interfaces* **2010**, *2*, 3406.
[24] B. Hui, F. Q. Huang, J. Liang, X. M. Xie, M. H. Jiang, *Adv. Mater.* **2011**, *23*, 3202.
[25] T. Q. Lin, F. Q. Huang, J. Liang, Y. X. Wang, *Energy Environ. Sci.* **2011**, *4*, 862.
[26] C. W. Jeong, P. Nair, M. Khan, M. Lundstrom, M. A. Alam, *Nano Lett.* **2011**, *11*, 5020.
[27] Y. Zhu, Z. Z. Sun, Z. Yan, Z. Jin, J. M. Tour, *ACS Nano* **2011**, *5*, 6472.
[28] T. Takahashi, H. Tokailin, T. Sagawa, *Phys. Rev. B: Condens. Matter* **1985**, *32*, 8317.
[29] H. Hibino, H. Kageshima, M. Kotsugi, F. Maeda, F. Z. Guo, Y. Watanabe, *Phys. Rev. B: Condens. Matter* **2009**, *79*, 125437.
[30] N. Romeo, A. Bosio, A. Romeo, *Sol. Energy Mater. Sol. Cells* **2010**, *94*, 2.
[31] P. K. Nayak, J. Bisquert, D. Cahen, *Adv. Mater.* **2011**, *23*, 2870.


© 2012 WILEY-VCH Verlag GmbH & Co. KGaA, Weinheim